JOURNAL OF APPLIED ELECTROCHEMISTRY **20** (1990) 723–727

Simultaneous solution of the potential equations for the metal and solution phases in cylindrical electrochemical reactors

J. M. BISANG

Programa de Electroquímica Aplicada e Ingeniería Electroquímica - (PRELINE),
Facultad de Ingeniería Química, Universidad Nacional del Litoral, Santiago del Estero 2829,
3000 Santa Fe, Argentina

Received 2 October 1989

The effect of the resistance of the metal phase on the current distribution in cylindrical electrochemical reactors taking into account the resistance of the solution phase is analyzed. A mathematical model is proposed, which assumes that the external electrode is isopotential and the electrochemical reaction on the external electrode has a low polarization resistance ($\mathrm{d}i/\mathrm{d}\eta \rightarrow \infty$). Consequently the equation for the potential distribution for the metal phase of the inner electrode was solved simultaneously with the Laplace equation for the solution phase. The theoretical current density distributions are compared with previous experimental results in order to determine the predictive suitability of the model and a good agreement is observed between them. Furthermore, a comparison is made between this model and an earlier one and a slight improvement in the prediction is observed.

Nomenclature

A_n	constant defined by Equation 25 (V)
A_n^*	constant defined by Equation 15 (V)
A_s	surface area per unit volume of electrode (cm^{-1})
E_0	reversible electrode potential (V)
$F(n)$	function defined by Equation 28 ($\mathrm{A\,cm}^{-1}$)
i	current density ($\mathrm{A\,cm}^{-2}$)
i_0	exchange current density ($\mathrm{A\,cm}^{-2}$)
I	total current (A)
I_k	modified Bessel function of the first kind of order k
j	$(-1)^{1/2}$
K_k	modified Bessel function of the second kind of order k
L	electrode length (cm)
n	index number in the series
r	radial coordinate (cm)
r_k	radius of k (cm)
R_n	function given by Equation 14, (V)
RT/F	constant (0.0257 V at 25° C) (V)
t	variable employed in the integration of Equations 23 and 24, (cm)
x	axial coordinate (cm)
X_n	function given by Equation 11
z	variable defined by $\mathrm{z} = \mathrm{j}\mu r$

Greek characters

α_c	charge transfer coefficient
γ_n	coefficient in the Fourier cosine series ($\mathrm{A\,cm}^{-2}$)
$\bar{\delta}_r$	mean relative deviation
η	overvoltage (V)
μ^2	separation constant in Equations 9 and 10 (cm^{-2})
ν_e	charge number of the electrode reaction
ρ	resistivity ($\Omega\,\mathrm{cm}$)
ϕ	potential (V)
$\phi_{s,n}$	function given by Equation 16 (V)

Subscripts

e	external electrode
i	internal electrode
m	metallic phase
s	solution phase

1. Introduction

The cylindrical geometry has many applications in industrial electrochemical systems. Cylindrical electrochemical reactors have been proposed for indirect electrosyntheses [1]. In this case, the useful species is generated at a large external electrode, being reconverted only partially at the thin inner electrode since its area is much smaller. Thus an undivided cell offering an appreciable cell voltage decrease and simplified constructive features can be applied. Since the central electrode experiences high current densities, when designing such units there is a need to take account of the distribution of the current density caused by the resistance of the metal and solution phases. A cylindrical geometry is also useful in equip-

0021-891X/90 $03.00 + .12

ment for protection against corrosion and for metal plating on tubes or wires.

In previous work carried out in this laboratory the experimental current distributions in cylindrical electrochemical reactors were determined using different test reactions and employing various methods of measurement. The experimental results were compared with those predicted by a model that considered only the resistance of the metal phase. It was concluded that when the modified Wagner number, dimensionless number originated in the mathematical solution of the model, exceeds 15×10^{-3} for concentrated solutions [2–3] the experimental results agree reasonably well with the values predicted by the model.

In order to predict more exactly the current distributions a second model was developed [4], which takes into account the resistance of the solution phase but assumes that the current at each axial position in the electrolyte is independent of the radial coordinate. The second model has a higher predictive capability than the former.

In the model reported here, the current in the electrolyte is a function of the axial as well as of the radial coordinate, consequently the current density distribution is obtained by simultaneous solution of the Laplace equation for the solution phase with the equation of the potential distribution for the metal phase of the inner electrode.

2. Mathematical model

The model assumes that: (a) the metal phase of the external electrode is isopotential. This electrode is easily accessed, therefore an electrical connection can be made in order to ensure isopotentiality; (b) the overvoltage at the external electrode is not a function of x; it is imperative that the electrochemical reaction has a high polarization curve slope ($\mathrm{d}i/\mathrm{d}\eta \rightarrow \infty$); (c) the changes in the reversible electrode potential with x are neglected.

Figure 1 shows schematically the geometry of the model. The radius of the external electrode is r_e. Considering that the inner electrode is a rod of length, L, and radius, r_i, fed at its lower end ($x = 0$), the differential current balance is given by

$$\frac{\mathrm{d}i_m(x)}{\mathrm{d}x} = -A_s i(x) \tag{1}$$

with

$$A_s = \frac{2}{r_i} \tag{2}$$

where $i(x)$ is the current density on the inner electrode at the position x.

Integrating Equation 1 with $i_m(0) = i_i$ and $i_m(L) = 0$ gives

$$i_i = A_s \int_0^L i(x)\,\mathrm{d}x \tag{3}$$

and i_i is given by

$$i_i = \frac{I}{\pi r_i^2} \tag{4}$$

Ohm's law for the metal phase may be written as

$$\frac{\mathrm{d}\phi_m(x)}{\mathrm{d}x} = -\rho_m i_m(x) \tag{5}$$

Differentiating Equation 5 with respect to x, and introducing Equation 1 yields

$$\frac{\mathrm{d}^2\phi_m(x)}{\mathrm{d}x^2} = A_s \rho_m i(x) \tag{6}$$

with the following boundary conditions:

$$x = 0 \quad \phi_m(0) = 0 \tag{6a}$$

$$x = 0 \quad \frac{\mathrm{d}\phi_m(x)}{\mathrm{d}x} = -\rho_m i_i \tag{6b}$$

The Laplace equation for the solution phase in cylindrical coordinates, neglecting the term of the angular coordinate, because of symmetry, is

$$\frac{\partial^2\phi_s}{\partial r^2} + \frac{1}{r}\frac{\partial\phi_s}{\partial r} + \frac{\partial^2\phi_s}{\partial x^2} = 0 \tag{7}$$

and the boundary conditions are

$$x = 0 \quad \frac{\partial\phi_s}{\partial x} = 0 \quad \text{for all } r \tag{7a}$$

$$x = L \quad \frac{\partial\phi_s}{\partial x} = 0 \quad \text{for all } r \tag{7b}$$

$$r = r_e \quad \phi_s(r_e, x) = 0 \quad \text{for all } x \tag{7c}$$

$$r = r_i \quad \frac{\partial\phi_s}{\partial r} = -\rho_s i(x) \tag{7d}$$

To obtain a solution by the method of separation of variables we set

$$\phi_s(r, x) = X(x)\,R(r) \tag{8}$$

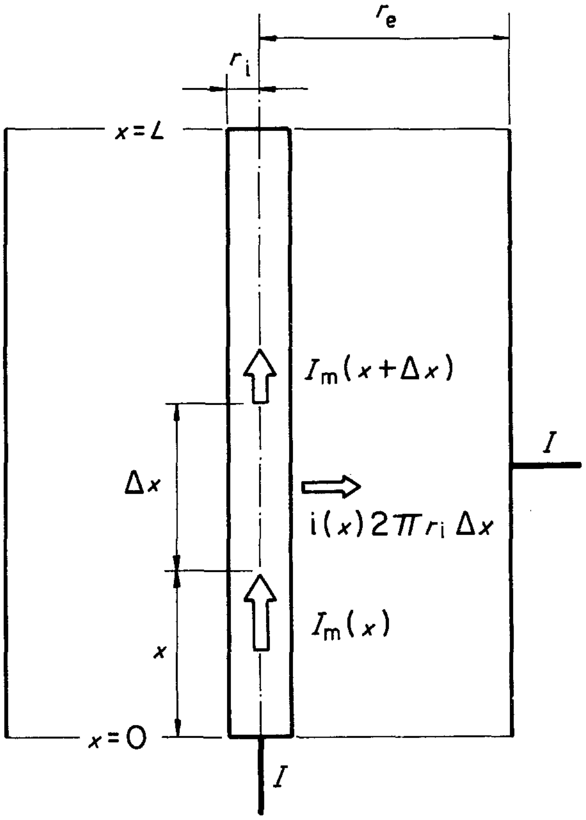

Fig. 1. Geometry of the model.

The differential equations for X and R are

$$\frac{\mathrm{d}^2X}{\mathrm{d}x^2} + \mu^2 X = 0 \qquad (9)$$

and

$$\frac{\mathrm{d}^2R}{\mathrm{d}r^2} + \frac{1}{r}\frac{\mathrm{d}R}{\mathrm{d}r} - \mu^2 R = 0 \qquad (10)$$

where μ^2 is the separation constant.

Considering the boundary conditions 7a and 7b, there are an infinite number of solutions of Equation 9 according to

$$X_n(x) = \cos\left(\frac{n\pi x}{L}\right) \ (n \text{ integral or zero}) \qquad (11)$$

being

$$\mu = \frac{n\pi}{L} \qquad (12)$$

By introducing the variable $z = \mathrm{j}\mu r$ Equation 10 is reduced to

$$\frac{\mathrm{d}^2R}{\mathrm{d}z^2} + \frac{1}{z}\frac{\mathrm{d}R}{\mathrm{d}z} + R = 0 \qquad (13)$$

a Bessel equation of zero order which has the solution

$$R_n(r) = A_n I_0\left(\frac{n\pi r}{L}\right) + A_n^* K_0\left(\frac{n\pi r}{L}\right) \qquad (14)$$

where I_0 and K_0 are the modified Bessel function of the first and second kind, respectively, of order zero; which are tabulated in [5]. Taking into account the boundary condition 7c is

$$A_n^* = -A_n\left[I_0\left(\frac{n\pi r_e}{L}\right)\Big/K_0\left(\frac{n\pi r_e}{L}\right)\right] \qquad (15)$$

Hence the functions $\phi_{s,n}(r, x) = R_n(r)X_n(x)$, at length

$$\phi_{s,n}(r, x) = A_n\left[I_0\left(\frac{n\pi r}{L}\right) - K_0\left(\frac{n\pi r}{L}\right)\left(I_0\frac{n\pi r_e}{L}\right)\Big/\left(K_0\frac{n\pi r_e}{L}\right)\right]\cos\left(\frac{n\pi x}{L}\right) \qquad (16)$$

are solutions of Equation 7, satisfying the boundary conditions 7a, 7b and 7c.

Clearly, a single solution $\phi_{s,n}(r, x)$ will, in general, not satisfy the boundary condition 7d. Now, since Equation 7 is linear and homogeneous, it follows that the sum of a finite number of solutions, $\phi_{s,n}(r, x)$, is a solution of Equation 7. To obtain a solution satisfying 7d, we consider the infinite series

$$\phi_s(r, x) = \sum_{n=0}^{\infty} A_n\left[I_0\left(\frac{n\pi r}{L}\right) - K_0\left(\frac{n\pi r}{L}\right)\left(I_0\frac{n\pi r_e}{L}\right)\Big/\left(K_0\frac{n\pi r_e}{L}\right)\right]\cos\left(\frac{n\pi x}{L}\right) \qquad (17)$$

Differentiating Equation 17 with respect to r, solving at $r = r_i$ and introducing Equation 7d yields

$$-\rho_s i(x) = \sum_{n=0}^{\infty} A_n\frac{n\pi}{L}\left[I_0'\left(\frac{n\pi r_i}{L}\right) - K_0'\left(\frac{n\pi r_i}{L}\right)\left(I_0\frac{n\pi r_e}{L}\right)\Big/\left(K_0\frac{n\pi r_e}{L}\right)\right]\cos\left(\frac{n\pi x}{L}\right) \qquad (18)$$

Considering the recurrence fomulae [15]:

$$I_0'\left(\frac{n\pi r_i}{L}\right) = I_1\left(\frac{n\pi r_i}{L}\right) \qquad (19)$$

and

$$K_0'\left(\frac{n\pi r_i}{L}\right) = -K_1\left(\frac{n\pi r_i}{L}\right) \qquad (20)$$

and introducing

$$\gamma_n = -\frac{A_n}{\rho_s}\frac{n\pi}{L}\left[I_1\left(\frac{n\pi r_i}{L}\right) + K_1\left(\frac{n\pi r_i}{L}\right)\left(I_0\frac{n\pi r_e}{L}\right)\Big/\left(K_0\frac{n\pi r_e}{L}\right)\right] \qquad (21)$$

into Equation 18 yields

$$i(x) = \sum_{n=0}^{\infty}\gamma_n\cos\left(\frac{n\pi x}{L}\right) \qquad (22)$$

Hence, in order that Equation 17 satisfies 7d, the coefficients γ_n must be chosen so that, for $r = r_i$, $1/\rho_s\ \partial\phi_s/\partial r\,|_{r_i}$ becomes the Fourier cosine series of $i(x)$, thus

$$\gamma_0 = \frac{1}{L}\int_0^L i(t)\,\mathrm{d}t \qquad (23)$$

and

$$\gamma_n = \frac{2}{L}\int_0^L i(t)\cos\left(\frac{n\pi t}{L}\right)\mathrm{d}t, \quad n = 1, 2, \ldots, \qquad (24)$$

By introducing Equation 24 into Equation 21 and solving for A_n yields

$$A_n = -\frac{2\rho_s\int_0^L i(t)\cos\left(\frac{n\pi t}{L}\right)\mathrm{d}t}{n\pi\left[I_1\left(\frac{n\pi r_i}{L}\right) + K_1\left(\frac{n\pi r_i}{L}\right)\left(I_0\frac{n\pi r_e}{L}\right)\Big/\left(K_0\frac{n\pi r_e}{L}\right)\right]} \qquad (25)$$

Likewise

$$A_0 = -\frac{\rho_s}{\pi}\int_0^L i(t)\,\mathrm{d}t \times \lim_{n\to 0} n^{-1}\left[I_1\left(\frac{n\pi r_i}{L}\right) + K_1\left(\frac{n\pi r_i}{L}\right)\left(I_0\frac{n\pi r_e}{L}\right)\Big/\left(K_0\frac{n\pi r_e}{L}\right)\right]^{-1} \qquad (26)$$

By introducing Equations 25 and 26 into Equation 17

$$\phi_s(r_i, x) = -\frac{\rho_s}{\pi}F(0) - \frac{2\rho_s}{\pi}\sum_{n=1}^{\infty}F(n)\cos\left(\frac{n\pi x}{L}\right) \qquad (27)$$

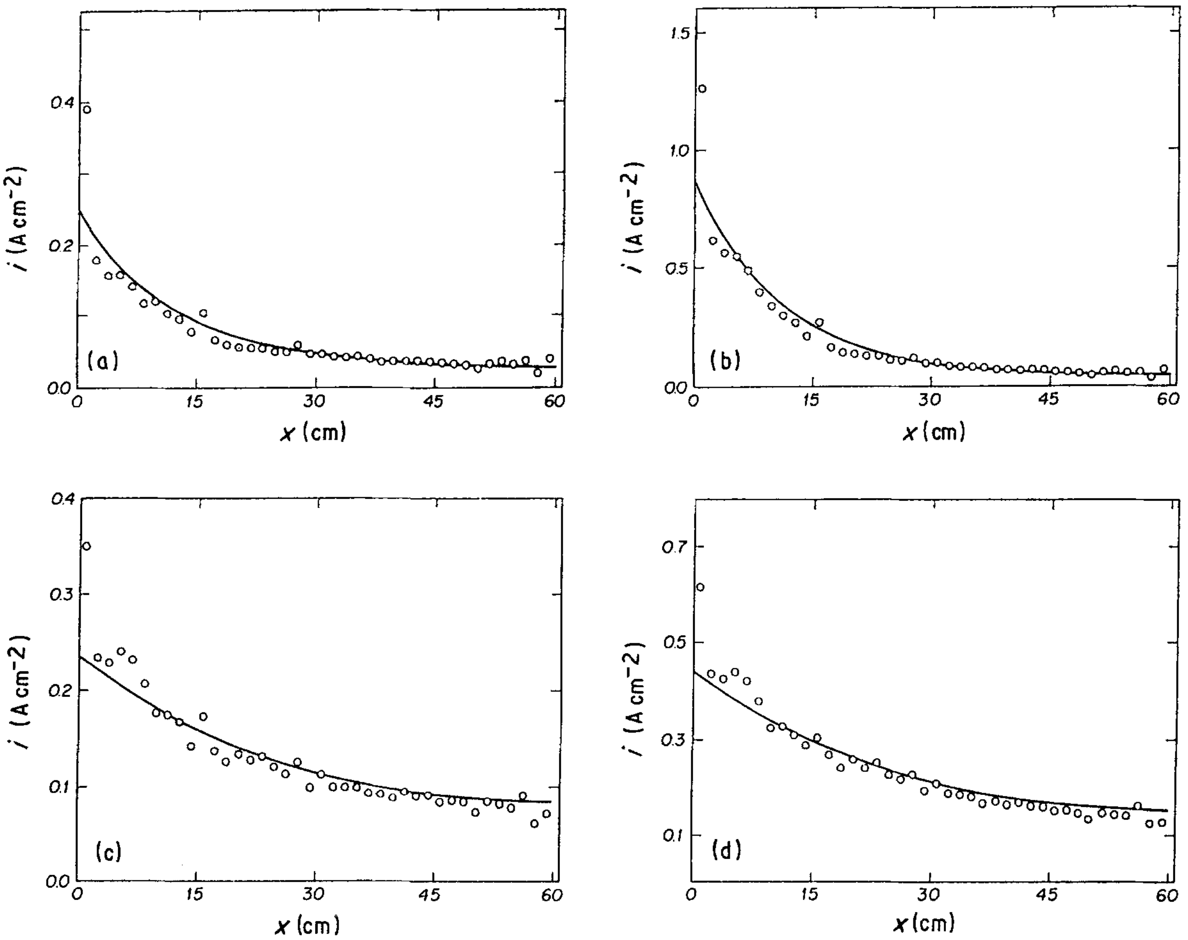

Fig. 2. Experimental (○) and theoretical (——) current distributions for hydrogen evolution. $T = 30°\,C$. (a) [NaOH] = 1 M, $I = 0.269\,A$; (b) [NaOH] = 1 M, $I = 0.727\,A$; (c) [NaOH] = 0.1 M, $I = 0.490\,A$; (d) [NaOH] = 0.1 M, $I = 0.896\,A$.

where

$$F(n) = \frac{\left[I_0\left(\frac{n\pi r_i}{L}\right) - K_0\left(\frac{n\pi r_i}{L}\right)\left(I_0\frac{n\pi r_e}{L}\right)\Big/\left(K_0\frac{n\pi r_c}{L}\right)\right]}{\left[I_1\left(\frac{n\pi r_i}{L}\right) + K_1\left(\frac{n\pi r_i}{L}\right)\left(I_0\frac{n\pi r_c}{L}\right)\Big/\left(K_0\frac{n\pi r_e}{L}\right)\right]n} \times \int_0^L i(t)\cos\left(\frac{n\pi t}{L}\right)\mathrm{d}t \qquad (28)$$

and

$$F(0) = \lim_{n\to 0} F(n) \qquad (29)$$

The definition of overvoltage is

$$\eta(x) = \phi_m(x) - \phi_s(r_i, x) - E_0 \qquad (30)$$

Taking into account Equation 27, η is expressed as

$$\eta(x) = \phi_m(x) + \left[\frac{\rho_s}{\pi}F(0) + \frac{2\rho_s}{\pi}\sum_{n=1}^{\infty}F(n)\cos\left(\frac{n\pi x}{L}\right)\right] - E_0 \qquad (31)$$

Finally

$$\eta(x) = \eta(0) + \phi_m(x) - \frac{2\rho_s}{\pi}\sum_{n=1}^{\infty}F(n)\left[1 - \cos\left(\frac{n\pi x}{L}\right)\right] \qquad (32)$$

For the electrochemical reaction at the inner electrode Tafel kinetics are assumed

$$i(x) = i_0 \exp\left[\frac{\alpha_c \nu_e F}{RT}\eta(x)\right] \qquad (33)$$

The current density distributions were obtained by simultaneous and iterative solution of Equations 3, 6, 28, 32 and 33. The solution of this system of equations was carried out numerically.

3. Results and conclusion

The experimental current density distributions were determined using the segmented counter electrode method. A detailed description of the equipment employed, method of operation, test reaction and reagents has been given previously in [2].

Figure 2 shows some typical current density curves as a function of position. Hydrogen evolution from alkaline solutions at 30° C was used as the test reaction. In each case, the full line represents the theoretical curve according to the model. It must be noted that there is a close agreement between the experimental and theoretical results.

In order to compare the predictive suitability of the present model and an earlier one [4], Table 1 shows the mean relative deviation, $\bar{\delta}_r$, of the experimental current densities with respect to the theoretical values for each model. The test reaction was hydrogen

Table 1. Review of the results (electrolyte: NaOH 1 *M; T* = 30° *C)*

I (A)	$\bar{\delta}_r \times 10^2$	
	This model	*Earlier model* [4]
0.1497	14.08	14.03
0.1736	17.30	17.18
0.2692	12.97	13.08
0.3915	13.31	13.43
0.4296	13.71	14.16
0.4859	13.82	14.10
0.5724	13.40	13.60
0.6393	14.63	14.94
0.7272	12.77	13.51
0.7574	12.54	13.19

evolution from 1 M NaOH solution. It can be seen that the new model shows a slight improvement in the prediction, the improvement being better for higher values of total current. However, for the hydrogen evolution from 0.1 M NaOH solution it was observed that both models present the same mean relative deviation.

Finally from this work it is concluded that the experimental results agree well with the predicted values and the new model has a higher predictive ability than the earlier one but at the expense of more computation time.

Acknowledgements

The author would like to thank Stiftung Volkswagenwerk and Deutscher Akademischer Austauschdienst (DAAD) of the Federal Republic of Germany for donating scientific equipment and Consejo Nacional de Investigaciones Científicas y Técnicas (CONICET), Argentina, for financial support of this work.

References

[1] A. J. Bellamy and B. R. Simpson, *Chem. Ind.* (London) (1981) 328.
[2] J. M. Bisang and G. Kreysa, *J. Appl. Electrochem.* **18** (1988) 422.
[3] J. M. Bisang, *Lat. Amer. Appl. Res.* **18** (1988) 63.
[4] J. M. Bisang, *J. Appl. Electrochem.* **19** (1989) 500.
[5] N. W. McLachlan, 'Bessel Functions for Engineers', 2nd Edn., Clarendon press, Oxford (1955).